JOURNAL OF CATALYSIS **164,** 387–398 (1997)
ARTICLE NO. 0395

Methane Reforming Reaction with Carbon Dioxide over Ni/SiO_2 Catalyst

II. A Mechanistic Study

V. C. H. Kroll, H. M. Swaan, S. Lacombe, and C. Mirodatos[1]

Institut de Recherches sur la Catalyse, CNRS, 2 Avenue Albert Einstein, F-69626 Villeurbanne Cédex, France

Received March 4, 1996; revised May 25, 1996; accepted August 9, 1996

The mechanism of the carbon dioxide reforming of methane was investigated over a nickel-on-silica catalyst. Non-steady-state and steady-state isotopic transient experiments combined with *in situ* DRIFT spectroscopy investigations were used to quantify the amount of the various adspecies present on the working catalyst surface. It was found that as soon as the catalyst is contacted with the reacting mixture, dehydrogenated carbon adspecies originating from the initial adsorption of methane and carbon dioxide are deposited on the nickel particles. Under steady-state reaction conditions, a permanent pool of adspecies equivalent to one monolayer of carbide-like species is continuously fed by the dissociative activation of gaseous methane. This initial activation step of methane is shown to be reversible, since it allows a fast CH_4/CD_4 exchange characterised by a marked isotopic effect. This pool of adspecies constitutes a reservoir of active carbon able to be oxidised into CO by oxygen atoms arising from the simultaneous carbon dioxide dissociation. This oxidation step which does not involve any C–H bond activation is assumed to be rate limiting since no kinetic isotopic effect is found for the formation of CO under the stoichiometric reforming conditions. Gaseous CO is also directly produced from the latter CO_2 dissociation. Adsorption/desorption equilibria ensure a fast interconversion between gaseous CO_2 and CO, as attested by their isotopic scrambling. A similar adsorption/desorption equilibrium is proposed for H_2O which, combined with the reversible activation of CO_2 and CO, leads to the achieved water–gas-shift equilibrium. Besides the rapid steps which constitute the catalytic cycle, slow side reactions involving the migration of the carbide-like species through the nickel particle and their transformation into structured coke or graphite growing as hollow whiskers are proposed to account for the ageing phenomena described in Part I of this work. A particular configuration of active sites is proposed on the basis of the main mechanistic statements.

INTRODUCTION

The reaction of methane reforming by carbon dioxide leading to synthesis gas with low H_2/CO ratios has recently gained a renewed interest within the general context of natural gas upgrading. Although noble metals have proved to be active and selective catalysts, ferrous metals (Fe, Co, and Ni) have been reported as a worthwhile alternative for this reaction (1). Some mechanistic approaches for noble metals have recently been published (2–4). However, to our knowledge no detailed mechanistic study over nonnoble metal catalysts has yet been reported.

In a general study of the CO_2 reforming over noble and ferrous metal catalysts, Rostrup-Nielsen and Bak Hansen (5) proposed that the reaction mechanism was unlikely to differ significantly from that of the steam reforming of methane. This statement was based on the fact that steam was also present in the CO_2 reforming process. Furthermore, operating conditions were estimated to be not too far from the steam reforming ones. This is in agreement with the previous conclusions of Bodrov and Apel'baum (6) following a kinetic study carried out on nickel foils in the temperature range 800–900°C. Their mechanistic proposals are summarised in Scheme IA, where the asterisk represents a surface site. According to this Scheme, CO_2 would dissociate into adsorbed O and gaseous CO while CH_4 would be stepwise activated into H_2 and CH_x adspecies. The latter would further react with the adsorbed oxygen to give CO. Like CO_2, H_2O would also be in equilibrium with the surface. Under the conditions of the CO_2 reforming, it is anticipated that the carbon monoxide would react with the surface into carbon adspecies, which could be less reactive than those arising from methane activation. This could explain the lower activities observed under CO_2 reforming than under steam reforming conditions for the same catalyst (5, 6).

Alternatively, Erdöhelyi *et al.* (7) and Mark and Maier (4) suggested that, at least on noble metals, carbon dioxide could also react directly from the gas phase with carbon adspecies arising from methane decomposition (Scheme IB).

The exact nature of the reacting intermediates arising from the two possible sources of carbon (i.e., methane and carbon dioxide) and their fate within the mechanistic scheme therefore remains an open fundamental question. From the point of view of catalyst and process development,

[1] To whom correspondence should be addressed. Fax: +33 472445399. E-mail: mirodato@catalyse.univ-lyon1.fr.

0021-9517/96 $25.00

A

$$CO_2 + {}^* = O^* + CO$$
$$CH_4 + {}^* = CH_3^* = CH_2^* = CH^* = C^*$$
$$CH_x^* + O^* = CO + x/2\ H_2 + 2^*$$
$$H_2O + {}^* = O^* + H_2$$
$$CO + 2^* = C^* + O^*$$

B

$$CH_4 + {}^* = C^* + 2\ H_2$$
$$C^* + CO_2 = 2\ CO + {}^*$$

SCHEME I

it is indeed of prime importance to determine the specific pathways leading either to the desired products, carbon monoxide and hydrogen, or to undesired compounds such as carbon dioxide, reversibly formed from CO or from accumulating carbonaceous deposits.

In order to clarify these points and to determine more precisely the relationship between the ageing of the catalyst and the reaction mechanism, a study was undertaken on a model catalyst, Ni/SiO_2, which was found to be active and rather stable for the CO_2 reforming of methane (8). Part I of this work (9) was focused on the ageing processes and the following conclusions were obtained:

(i) Whatever the pretreatment of the catalyst, a carbide-like surface formed instantaneously, presenting a catalytic activity little dependent on the particle morphology and the degree of nickel reduction.

(ii) During time-on-stream, slight particle sintering occurred and various forms of coke accumulated outside the particles.

(iii) In contrast to the reforming activity, the coke formation appeared to be highly dependent on the pretreatment conditions. A reduction under the reaction conditions tended to produce essentially nontoxic or little toxic filamenteous carbon, while a prereduction under hydrogen tended to produce highly toxic encapsulating carbon.

(iv) At temperatures lower than 700°C, less particle sintering but considerably higher rates of coke deposition were observed, in agreement with thermodynamic considerations. In this case the deactivation rates tended to be independent of the catalyst pretreatment and morphology.

(v) Finally, the optimised conditions for catalyst stability were obtained without prereducing the catalyst and operating at a temperature of 700°C in a reactor where temperature gradients were minimised.

The present study reports transient kinetics experiments (without and with isotopic labeling) and surface characterisation under the reaction conditions by *in situ* diffuse reflectance infrared Fourier transform (DRIFT) spectroscopy aimed at identifying the carbon pathways in the mechanistic scheme (10).

EXPERIMENTAL

Catalyst preparation and pretreatment. The Ni/SiO_2 catalyst was prepared by wet impregnation of a Degussa Aerosil P200 support with $Ni(NH_3)_6NO_3$ solution as already described (11). This catalyst has already been tested thoroughly for the CO_2 reforming reaction, as previously reported. It was found that the best catalyst stability was achieved after precursor calcination at 750°C for 8 h under flowing oxygen. After calcination the catalyst pellet size was brought to 0.2–0.3 mm, unless otherwise specified. However, it was also shown that the catalyst sample was reduced on stream by the reaction mixture itself. In order to avoid this initial evolution of the catalyst a reduction step was performed after calcination for the present mechanistic investigation. The catalyst was loaded into a tubular quartz reactor and subsequently reduced *in situ* at 750°C for 10 h under pure hydrogen (flow rate, 1.2 liters/h; temperature rise, 2.5°C/min). The external thermocouple was located at the same level as the catalyst bed. The microreactor had an internal diameter of 4 mm.

Mechanistic experiments. Steady-state experiments aimed at determining kinetic isotope effects (KIE) were performed at 700°C and at atmospheric pressure by feeding the reactor with the mixtures $CH_4/CO_2/Ar$ or $CD_4/CO_2/Ar$ (7.5/7.5/85). Various contact times were used in order to measure the KIEs at different conversion levels. Experiments aimed at determining the H/D exchange of methane were carried out by feeding an equimolar mixture of light and deuterated methane $CH_4/CD_4/CO_2/Ar$ (3.75/3.75/7.5/85) with a total flow rate equal to 3 liters/h.

Furthermore, transient experiments were performed at 700°C by abruptly switching the inlet feed to one with a different gas composition (non-steady-state transient kinetics) or with a different isotopic composition (steady-state isotopic transient kinetic analysis (SSITKA)) (10). Argon was used as an inert tracer and helium as balance. The total flow rate was 3 liters/h. Table 1 reports the changes in feed compositions and the time intervals between two consecutive transients carried out on a fresh sample. Typically, the

TABLE 1

Feed Composition Switches during Transient Experiments at 700°C

Initial mixture CH_4/CO_2/He	Time interval (min)	Switch to mixture CH_4/CO_2/(He + Ar)	Time interval (min)	Switch to mixture CH_4/CO_2/He
00/00/100	0.5	15/15/70	30	00/00/100
15/15/70	0.5	00/15/85	2	15/15/70
15/15/70	0.5	15/00/85	2	15/15/70
$^{12}CH_4/^{12}CO_2$/He		$^{13}CH_4/^{12}CO_2$/He		$^{12}CH_4/^{12}CO_2$/He
9.5/9.5/81	0.5	9.5/9.5/81	0.5	9.5/9.5/81

reactor was loaded with 26.0 mg of Ni/SiO_2, diluted with 34.1 mg quartz.

The product streams were analysed by gas chromatography (GC) (Delsi 200, equipped with a TCD detector and a Carbosieve SII column) for steady-state experiments and by on-line mass spectrometry (MS) (VG Pegasus) for non-steady-state experiments. Coupled GC/MS analysis was used in the case of the H/D exchange steady-state experiments. The following gases were used: CH_4 (Alpha gaz, purity > 99.995%), He (Carboxyque France, purity > 99.998%), CO_2 (Alpha gaz, purity > 99.995%), $^{13}CH_4$ and CD_4 (Bureau des Isotopes Stables, France), Ar (Air Liquide, purity > 99.995%).

Catalyst characterisation. A flash temperature programmed oxidation (TPO) experiment was carried out over 24.6 mg of catalyst aged for 10 min at 700°C under a mixture of $^{13}CH_4/^{12}CO_2$/He (9.5/9.5/81), with a flow rate of 3 liters/h. While purging with helium the reactor was cooled down to room temperature. The oxidising mixture was admitted to the catalyst (O_2/He (20/80); flow rate, 3 liters/h) and the temperature was rapidly raised to 700°C by placing the reactor in the furnace preheated at 700°C (which corresponded to a mean heating rate of 140°C/min). The gases were analysed by on-line mass spectrometry. The desorption peaks, corrected for background and fragmentation, were decomposed and integrated. The corresponding amounts were determined after proper calibration of the mass spectrometer.

The infrared measurements were performed using a Nicolet 550 spectrometer, equipped with an *in situ* DRIFT cell (Spectratech). Data were automatically collected and sent to a personal computer for acquisition and data analysis. Typically the undiluted catalyst loading was 20 mg with a pellet size of 0.1–0.2 mm. The sample was reduced *in situ* as described previously. The reaction was carried out at either 500 or 700°C with a feed consisting of 15 vol% CH_4, 15 vol% CO_2, and argon as diluent (total flow rate, 3.0 liters/h). After reaction at 700°C, a TPO was carried out in a stream of 20 vol% O_2 and 80 vol% Ar (total flow rate, 3.0 liters/h). All the spectra were taken with a resolution of 4 cm^{-1} and a KBr spectrum was used for background. Spectra taken at 700°C after catalyst reduction and Ar flush were considered as reference and subtracted to the spectra obtained under reaction conditions in order to identify the surface species arising from the reaction itself.

RESULTS

State of the Catalyst Used for the Mechanistic Investigations

From the detailed characterisation study reported in Part I (9), the Ni/SiO_2 catalyst used for the present mechanistic investigations can be described as reduced with a dispersion of the nickel phase of 17%. This corresponded to a mean particle size of 63 Å, with a rather narrow size distribution. The morphological state of the solid was assumed to be stable during the mechanistic experiments, since their duration was kept small compared to the deactivation rate by sintering.

Rate of Methane and Carbon Dioxide Conversion under Steady-State Conditions

After the activation procedure described above, the reaction rate of methane and carbon dioxide measured at 700°C after 1 h on stream was 2.1 and 2.4 mol/h/g_{cat}, respectively, with a selectivity towards CO and H_2 of 95 and 92%, respectively.

Measurement of Kinetic Isotopic Effects (KIE)

Steady-state experiments were also performed under similar reaction conditions with perdeuterated (CD_4) instead of light (CH_4) methane in order to measure kinetic isotopic effects. Experimental KIEs were directly obtained from the ratio of methane or carbon dioxide conversion levels corresponding to CH_4 and CD_4 feeds. The corresponding data relating to two sets of experiments carried out at 700°C with different contact times are reported in Table 2. As can be seen, no significant KIE was found either for the methane or for the carbon dioxide conversion, whatever the degree of conversion. The theoretical KIE expected if a C–H bond breaking was rate determining was calculated according to the simplified formulas reported in Ref. (12), which gave a value close to 1.8 at 700°C.

Measurement of the Rate of H/D Equilibration

The rate of H/D equilibration under reforming conditions was evaluated by replacing the methane inlet feed by an equimolar CH_4/CD_4 mixture. Table 3 reports the isotopic composition of fed methane at the reactor inlet and of the nonreacted methane and of the produced hydrogen at the reactor outlet. From the mean number of H and D per methane molecule found in the experimental isotopic distribution, the isotopic composition which would correspond to a random distribution of the H and D atoms was

TABLE 2

Kinetic Isotopic Effects (KIE) Measured at 700°C for Two Sets of Experiments A and B Carried out at Different Contact Times, 0.33g · mol/h and 0.17 g · mol/h, Respectively

	Methane conversion		Carbon dioxide conversion	
Feed	A	B	A	B
CH_4/CO_2/Ar (%)	84.7	43.3	89.5	54.3
CD_4/CO_2/Ar (%)	84.6	45.3	92.7	59.4
KIE	1.00	0.96	0.97	0.92

TABLE 3

Experimental and Statistical Isotopic Distribution of Gaseous Methane and Hydrogen Measured at 700 and 600°C, Corresponding to an Equimolar CH_4/CD_4 Inlet Mixture with CO_2

	T (°C)	$X_{methane}$ (%)	Methane distribution (%)					Hydrogen distribution (%)		
			CH_4	CH_3D	CH_2D_2	CHD_3	CD_4	H_2	HD	D_2
Experimental (inlet)			49.5	0.3	0.1	0.5	49.6	—	—	—
Statistical[a]			6.2	24.8	37.5	25.2	6.3			
Experimental (outlet)	700	89	0.1	22.5	45.1	19.7	12.6	24.6	48.4	27.0
Statistical			3.9	19.5	36.6	30.5	9.5	23.7	50.0	26.3
Experimental (outlet)	600	35	40.7	0.6	0.3	1.3	57.1	32.7	29.1	38.2
Statistical			3.0	16.8	35.4	33.1	11.7	22.3	49.8	27.9

[a] Statistical distribution calculated by assuming that the H and D atoms found in the experimental distribution are randomly distributed.

also calculated according to the binomial formula (10). The overall methane conversion is also reported. It can be seen that:

(i) The ratio of exchanged methane (i.e., the sum of the CH_3D, CH_2D_2, and CHD_3 outlet partial pressures) to the total amount of converted methane (into CO/CO_2) was equal to 0.10 and 0.04 at 700 and 600°C, respectively. These values indicated that the probability for an activated methane to be converted was much higher than its probability to be recombined into gaseous methane, at both temperatures. In other words, the overall methane conversion appeared to be largely irreversible.

(ii) The experimental distribution of the unconverted methane at the reactor outlet tended to be statistical at 700°C, while a much reduced exchange was observed at 600°C. This means that a large and fast gas/surface equilibrium established at 700°C for the unconverted fraction of methane. However, a clear shift of the isotopic distribution towards the heavier methanes (indicating that the mean number of D atoms per methane molecule was larger than the number of H atoms) was observed. This indicated that the recombination of surface species into heavy methanes was much more likely than the recombination into light methane. This demonstrated a marked KIE for the methane reversible activation, as expected for steps which indeed implied C–H (or C–D) bond activation.

(iii) The isotopic composition of produced hydrogen was very close to the statistical one at 700°C, indicating a fast gas/surface exchange for hydrogen, without marked isotopic effect (almost symmetrical distribution). The latter indicated that this equilibrium did not involve slow C–H or O–H bond activation. At 600°C, a smaller degree of exchange was observed (around 60%), but still much larger than the CH_4/CD_4 one observed at the same temperature.

(iv) No data are reported for water due to the poorly resolved GC/MS related signals. However, qualitative evidence of isotopic scrambling was also obtained.

Nonstationary Kinetic Experiments

$He \rightarrow CH_4/CO_2/He/Ar$. The first transient $He \rightarrow CH_4/CO_2/He/Ar$ was performed on a fresh, nonreacted sample (Fig. 1). The order of gas appearance at the reactor outlet was H_2, CO, Ar, then CH_4 and CO_2 together, and finally H_2O, significantly delayed. From the observed delay between the Ar response (which corresponds to the noncatalytic system response) and the CH_4 and CO_2 responses, it was deduced that an initial CH_4 and CO_2 uptake occurred on the clean catalyst surface. This initial adsorption, calculated from the product of the integrated delays (time units) and the flow rate of the considered gases,

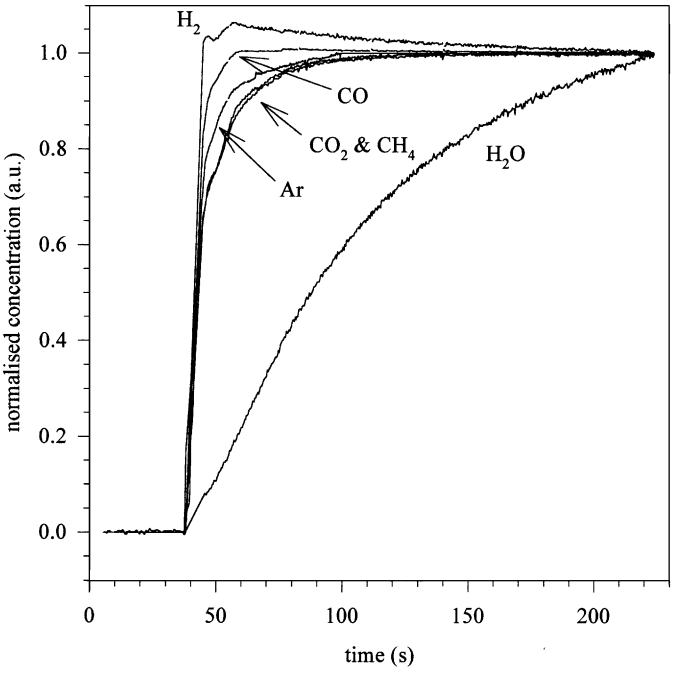

FIG. 1. Normalised responses after the transient $He \rightarrow CH_4/CO_2/He/Ar$ at 700°C.

TABLE 4

Amounts of Adsorbed (^{A}) and Desorbed (^{D}) Species Measured during the Transient Experiments Carried out at 700°C

Transient steps	CH_4[a]	CO_2[a]	CO[a]	H_2[a]	Total I/Ni_s^0
$He \rightarrow CH_4/CO_2/He/Ar$	160^A (2.2)	130^A (1.5)	120^D (1.3)	400^D	2.4
$CH_4/CO_2/He/Ar \rightarrow CO_2/He$	14^D (0.2)	—	514^D (5.8)	—	6.0
$CH_4/CO_2/He/Ar \rightarrow CH_4/He$	820^A (9.3)	—	—	1538^D	9.3
$^{12}CH_4/^{12}CO_2/He \rightarrow {}^{13}CH_4/^{12}CO_2/He/Ar$	ϵ[b]	7^A (0.10)	38^A (0.43)	—	0.53

Note. The corresponding atomic ratios I/Ni_s^0 reported in brackets were calculated from the amounts of adsorbed and desorbed species and from the nickel dispersion determined by magnetic measurements.

[a] Data in $\mu mol/g_{cat}$ (I/Ni_s^0).

[b] ϵ means not accurately measurable.

corresponded to 160 $\mu mol/g_{cat}$ for CH_4 and 130 $\mu mol/g_{cat}$ for CO_2 (Table 4). In contrast, the appearance of H_2 and CO before the inert tracer indicated an initial release of hydrogen and carbon monoxide (estimated at around 400 and 120 $\mu mol/g_{cat}$, respectively). From this simultaneous occurrence of CH_4/CO_2 uptake and H_2/CO release, it may be assumed that during this start-up period the adsorbed methane was dehydrogenated into evolving hydrogen and deposited carbon, while the CO_2 uptake led to gaseous CO and adsorbed oxygen since no gaseous oxygen was detected during this transient experiment. Water was also slowly released from the catalyst, as indicated by the marked delay observed in Fig. 1. No precise quantification of water uptake or release was performed because a significant part of this delay originated from a chromatographic effect along the set-up lines, as revealed by blank experiments carried out in the presence of water introduced in the inlet flow.

$CH_4/CO_2/He/Ar \rightarrow CO_2/He$. When only methane was abruptly suppressed from the reacting mixture (transient $CH_4/CO_2/He/Ar \rightarrow CO_2/He$, Fig. 2) the CO_2 response increased rapidly as expected from the decrease of conversion. However, the disappearance of CO was now delayed compared to Ar and H_2, showing that CO_2 was able to react with adspecies to form CO. This residual production of CO under the CO_2/He mixture amounted to around 514 $\mu mol/g_{cat}$. Once more methane was only slightly delayed, representing 14 $\mu mol/g_{cat}$. Note that besides the residual formation of CO no other products were detected under CO_2/He atmosphere except water, desorbing very slowly, almost symmetrically to its initial slow appearance. The latter confirmed the previous remark concerning the chromatographic effect on the water response. The catalyst was exposed to the CO_2/He mixture for 2 min before methane was readmitted again. After reaching steady state, a decrease in catalyst activity of around 15% was observed.

$CH_4/CO_2/He/Ar \rightarrow CH_4/He$. When carbon dioxide was abruptly suppressed from the reacting mixture (Fig. 3), CO disappeared rapidly together with CO_2. However, after

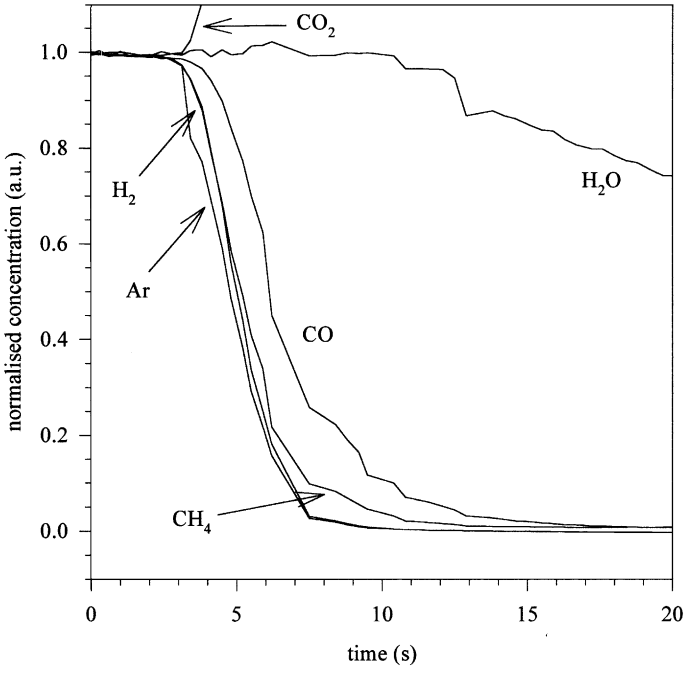

FIG. 2. Normalised responses after the transient $CH_4/CO_2/He/Ar \rightarrow CO_2/He$ at 700°C.

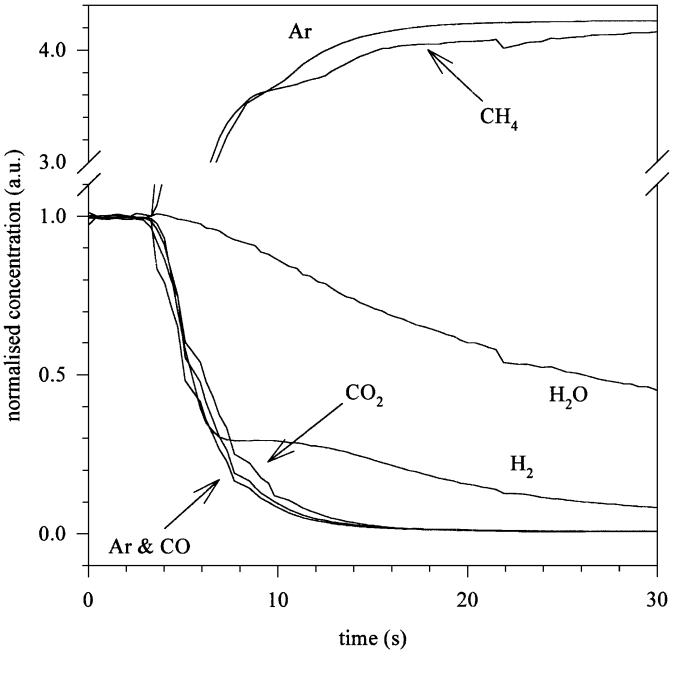

FIG. 3. Normalised responses after the transient $CH_4/CO_2/He/Ar \rightarrow CH_4/He$ at 700°C.

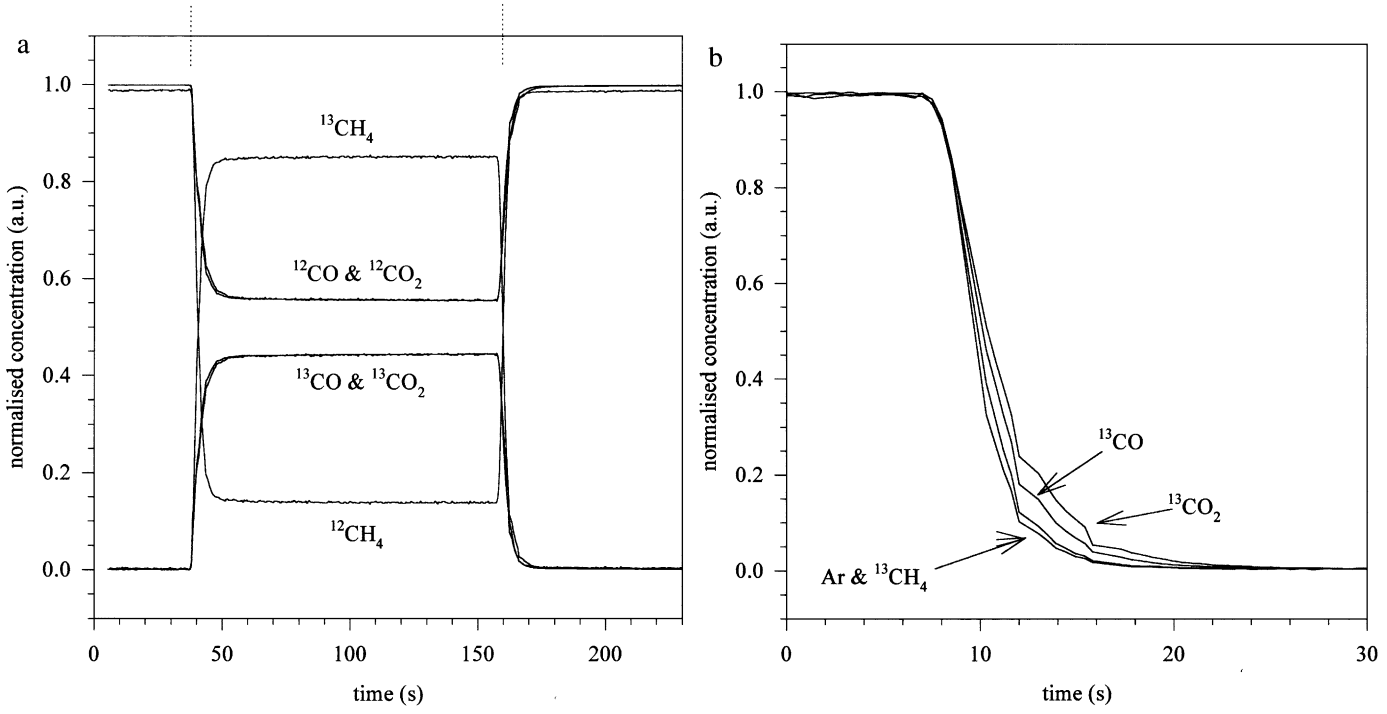

FIG. 4. (a) Normalised responses corresponding to the transients $^{12}CH_4/CO_2/He \rightarrow {}^{13}CH_4/CO_2/He/Ar \rightarrow {}^{12}CH_4/CO_2/He$ at 700°C. (b) Normalised responses after the transient $^{13}CH_4/CO_2/He \rightarrow {}^{12}CH_4/CO_2/He/Ar$ at 700°C.

an initial fast decrease the H_2 signal relaxed slowly to zero during the 2-min transient period. This delayed production of H_2 was estimated at around 1538 μmol/g_{cat}, which was almost four times the amount of hydrogen released during the initial catalyst start-up (Table 4). This residual but lasting production of hydrogen corresponded to a residual conversion of methane during the same period, evaluated to 820 μmol/g_{cat} by comparison with a reference signal (Ar signal at top of Fig. 3) representing the concentration of methane in the absence of reaction. After 2 min under CH_4/He atmosphere the inlet flow was switched back to the initial reacting mixture CH_4/CO_2/He/Ar. The initial steady-state catalyst activity was fully recovered, at variance with the deactivation observed above after the transient period under CO_2/He atmosphere.

This treatment of the catalyst under methane/helium atmosphere was also studied in a reactor allowing *in situ* magnetic measurements (9). A calcined sample was aged for 4 h at 700°C under reacting mixture, leading to 95% of ferromagnetic nickel, in agreement with the data reported in Part I (9). Then the sample was treated at the same temperature for 1 h under CH_4/He flow: a marked decrease of the ferromagnetic signal was observed (from 95 to 68%), which indicated that a significant part of the nickel phase reacted with methane to form nonferromagnetic compounds under methane-rich atmosphere. A temperature programmed hydrogenation (TPH) experiment was then carried out by exposing the reacted sample to a pure hydrogen flow from room temperature to 325°C (9). The final TPH temperature was chosen in order to restrict the hydrogenation to the most reactive carbonaceous deposits as shown in Part 1 of the present study (see Table 2 in Ref. (9)): 100% of ferromagnetic Ni was obtained after this temperature restricted TPH. This result demonstrated unambiguously that under methane-rich atmosphere, the nickel particles partly reacted with carbon species to form a new phase which was not ferromagnetic, the formation of the latter being easily reversible under hydrogen flow at moderate temperature.

Steady-State Isotopic Transient Experiment

$^{12}CH_4/^{12}CO_2/He \rightarrow {}^{13}CH_4/^{12}CO_2/He/Ar \rightarrow {}^{12}CH_4/^{12}CO_2/He$. The isotopic switches under overall steady-state conditions led to the transient responses reported in Figs. 4a and 4b. Table 5 reports the isotopic composition of the effluent

TABLE 5

Isotopic Composition of the Effluents at 700°C when the Reactor was Fed with the $^{13}CH_4/^{12}CO_2$/He/Ar mixture

	^{12}C (%)	^{13}C (%)
CH_4	14	86
CO_2	56	44
CO	56	44

gases after the first switch, i.e., when the reactor was fed with the $^{13}CH_4/^{12}CO_2$/He/Ar mixture.

As can be seen from Fig. 4a and Table 5, the isotopic composition of the unconverted CO_2 after the switch $^{12}CH_4/^{12}CO_2$/He $\rightarrow$ $^{13}CH_4/^{12}CO_2$/He/Ar was almost equilibrated between $^{12}CO_2$ and $^{13}CO_2$ (respectively 56 and 44%), while only $^{12}CO_2$ was fed into the reactor. The produced CO presented exactly the same isotopic composition. In contrast, much less isotopic scrambling was observed for the outlet methane with 86% $^{13}CH_4$ and 14% $^{12}CH_4$ at the reactor outlet, while only $^{13}CH_4$ was fed into the reactor.

The normalised responses of each labeled gas were calculated referring to their steady-state compositions before and after the switches. Figure 4b reports the normalised decay of the ^{13}C molecules during the second switch, as an example. The symmetrical curves observed simultaneously for the ^{12}C molecules are omitted for sake of clarity. Similar curves were obtained during the first isotopic switch. Almost no significant delay was observed between the response of the labeled methane and the argon tracer representing the reference signal. This indicated that no adsorbed molecular methane was reversibly accumulating under steady-state conditions. In contrast to methane, a significant delay was observed for the CO_2 signal, clearly indicating that carbon dioxide was reversibly interacting with the catalyst surface under steady-state conditions. Quantitatively, this delay was estimated to be around 0.88 s (an average value obtained from several isotopic transients). Considering the CO_2 concentration at the reactor outlet, this led to an accumulation of around 7 μmol/g_{cat} of reversibly adsorbed CO_2 (Table 4). Note that this amount represented only 1/20th of the initial CO_2 irreversible adsorption observed during the catalyst start-up (130 μmol/g_{cat}).

The delay observed between the Ar reference signal and the produced ^{13}CO was estimated to be $\tau_{CO} = 0.48$ s (Fig. 4b). An estimation of the amount of the CO precursors was obtained from the product of the steady-state rate of methane conversion and the delay τ_{CO} (10). A value of 38 μmol/g_{cat} was thus determined.

Flash TPO

Figure 5 reports the concentration of carbon dioxide produced during a TPO experiment carried out after an ageing period of 10 min under $^{13}CH_4/^{12}CO_2$/He stream at 700°C (the conversion of methane was 74% and of carbon dioxide 84%). After spectrum decomposition, two peaks of CO_2 were observed for both $^{12}CO_2$ (amu 44) and $^{13}CO_2$ signals (amu 45): there was a sharp one at around 500°C and a broad one, badly resolved, with a maximum at around 650°C. Table 6 gives the amount of formed CO_2 and the respective isotopic composition. The low temperature peak was predominantly formed of ^{13}C (76%), while the broad high temperature peak presented a higher concentration in ^{12}C (60%).

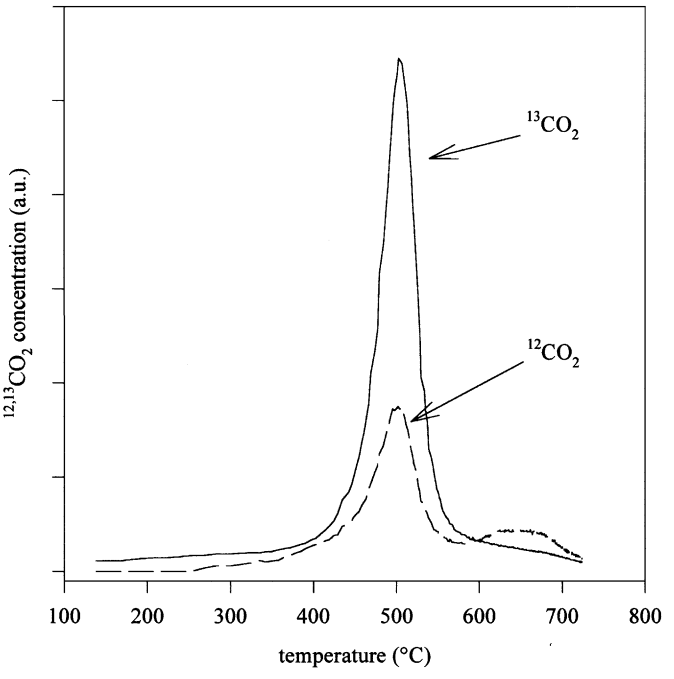

FIG. 5. CO_2 produced during flash TPO performed after a 10-min run at 700°C with a $^{13}CH_4$ and $^{12}CO_2$ feed.

Let us recall that during nonisotopic TPO experiments, already reported in Ref. (8), similar CO_2 peaks were observed, namely a first one already appearing after a very short ageing period (as for the above case) with a maximum at around 350°C, and a second one developing under reaction with a maximum shifting from 700 to 600°C with time-on-stream.

In Situ FT-IR Investigations

Figure 6 reports the DRIFT spectra obtained under reaction conditions at 500 and 700°C after subtraction of the reference spectra taken after reduction and flushing with argon. Figure 7 reports the changes in band intensities with time-on-stream at 500°C, time zero corresponding to the switch from Ar to the reacting mixture before feeding the DRIFT cell. The results show the following:

(i) At 500°C (Figs. 6a and 7) a well defined band at 3718 cm^{-1} appeared rapidly on the working surface within

TABLE 6

Amount and Isotopic Composition of the Carbon Dioxide Formed during TPO of a Catalyst Aged for 10 Min under $^{13}CH_4/^{12}CO_2$/He Stream at 700°C

TPO peak temperature (°C)	Absolute amounts (μmol/g_{cat})		Isotopic composition (%)	
	$^{12}CO_2$	$^{13}CO_2$	^{12}C	^{13}C
500	11.6	35.6	24	76
650	24.8	12.8	60	40

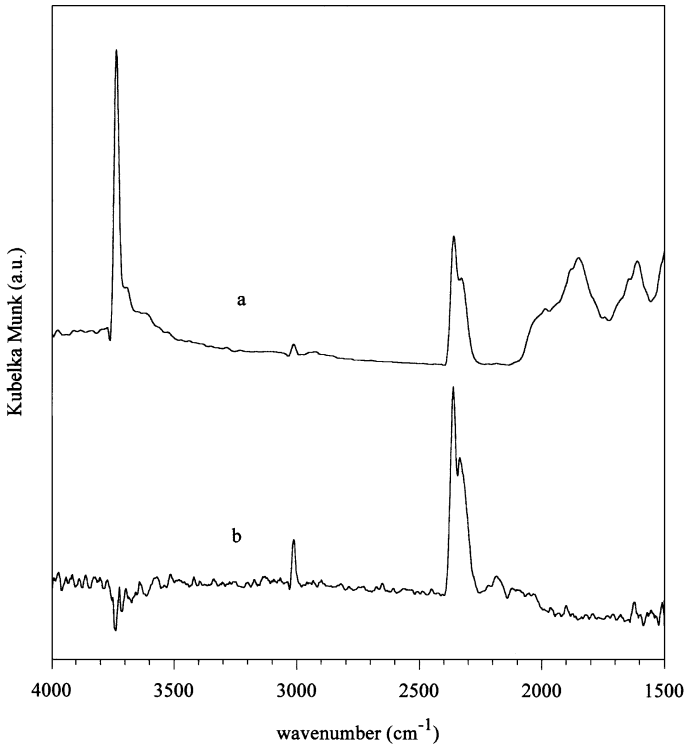

FIG. 6. *In situ* FT-IR spectra under reaction conditions at (a) 500 and (b) 700°C.

2 min after contacting the catalyst with the reacting mixture. This band corresponds clearly to terminal silanol groups Si–OH, already present on the reduced sample, and not to Ni–OH groups which were found on bulk nickel hydroxide to absorb at 3707, 3682, and 3641 cm^{-1} (13). This means that water initially formed on the nickel active phase was trapped by the silica support. The stabilisation of the band intensity corresponds most probably to the saturation of the surface capacity to accommodate hydroxyl groups at 500°C. Within the same initial start-up period intense bands developed at 2012 and 1855 cm^{-1}. These two bands can be assigned to CO adsorbed species, linear and multibonded, respectively, as reported for CO_2 adsorption on similar Ni/SiO_2 catalysts (13). Besides these adsorbed species, a gas phase contribution was observed at 3050 cm^{-1} for CH_4 and at 2359 and 2330 cm^{-1} for CO_2. Note that under these conditions the methane and carbon dioxide conversions were very low, approximately 1% as checked by on-line MS analysis. This was attested by a very weak CO gas doublet on the DRIFT spectra (Fig. 6a). It can also be stressed that within the rather poor time resolution of the spectrum acquisition, the appearance of adsorbed CO species was not delayed but even anticipated the appearance of CH_4 and CO_2 gas phase bands, which corresponded well to the fast initial CO gas formation observed on the previously reported transient experiments (Fig. 7).

(ii) At 700°C, i.e., under the reaction conditions prevailing in the present study, a complete change in the surface occupancy was observed: no hydroxyl bands, nor adsorbed CO species developed on the working surface (Fig. 6b). Due to a much higher methane conversion (around 16%), the doublet of gaseous CO was now clearly detected at 2175 and 2115 cm^{-1}. It was also observed that during time-on-stream several broad and weak bands developed slowly in the 2700–3000 cm^{-1} range, superimposed on the absorption vibrations of gaseous CH_4. The IR beam absorption by the sample was also found to increase with time-on-stream, resulting in a decreased signal/noise ratio. After 22 h on stream, only a residual signal could be collected.

A detailed spectrum of the C–H bands developing slowly with time-on-stream was obtained after flushing the reacting gas phase with argon after 22 h on stream, as reported in Fig. 8a. Although weak and poorly resolved, the main bands around 2965, 2928, and 2860 cm^{-1} can be assigned to asymmetric and symmetric stretching vibrations of $–CH_3$ and $=CH_2$ species. A weak shoulder at around 2890 cm^{-1} also suggests the presence of some $\equiv CH$ groups (14).

In situ TPO of the reacted sample was carried out after cooling down the DRIFT cell to room temperature under argon flow and subsequently heating it under oxygen flow up to 750°C at 2°C/min. The CH bands described above disappeared between 700 and 750°C restoring the reference spectrum after reduction. This observation strongly suggests that the extinction phenomenon observed under reaction conditions was due to carbon deposition and that

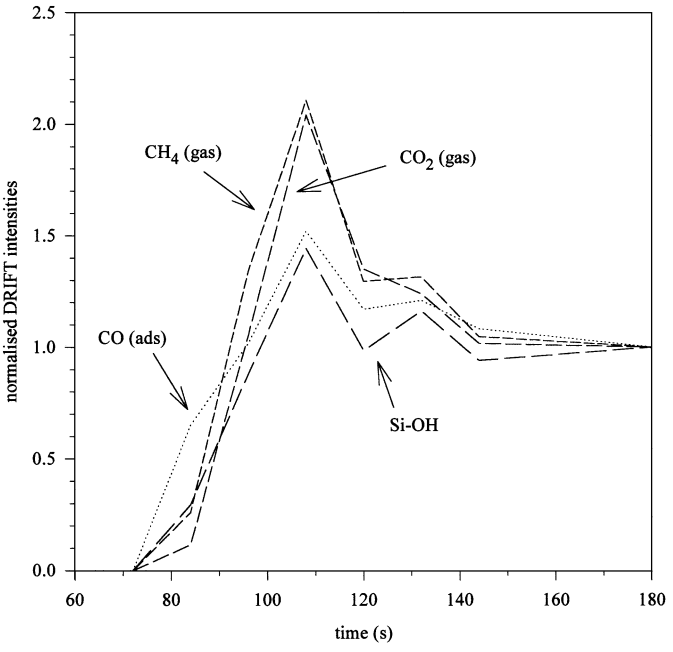

FIG. 7. DRIFT signal intensities of adsorbed species and gas phase components after the transition $Ar \rightarrow CO_2/CH_4/Ar$ as a function of time at 500°C.

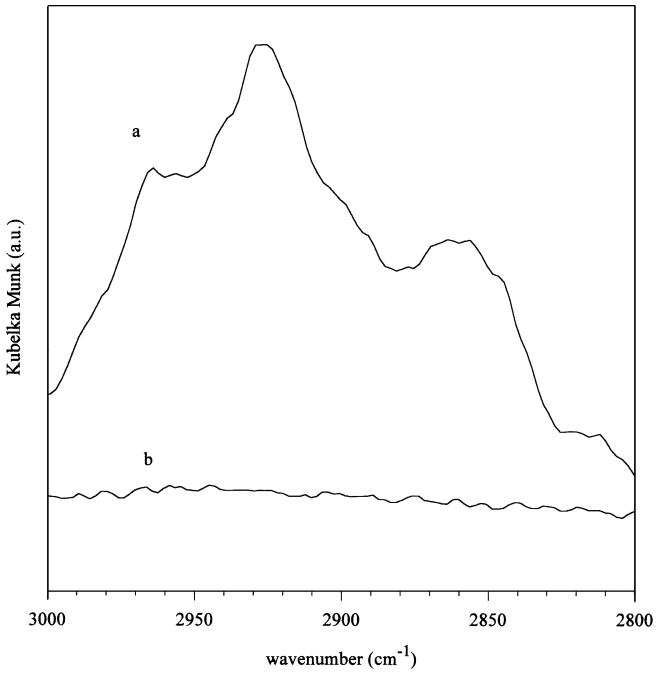

FIG. 8. Spectral detail of C–H absorption band region under reaction conditions (a) after 22 h of reaction, (b) after a TPO up to 750°C.

the restoring of the signal during TPO corresponds to the oxidation of these carbonaceous deposits. From the temperature range corresponding to the oxidation of these carbon deposits (between 700 and 750°C), it may be deduced that the above-described hydrogenated carbon adspecies represented stable deposits. Consequently, they cannot be ascribed to any of the reacting adspecies immediately available on the reacting surface.

DISCUSSION

Part I of the present study was focused on the ageing phenomena occurring during the CO_2 reforming on Ni/SiO_2 catalysts. Besides the morphological changes in nickel particles induced by sintering processes, the analysis of carbon deposition by combined magnetic measurements and TPH experiments with time-on-stream revealed that several types of carbon deposits could be considered. It was shown that the Ni particles contacted with the reacting mixture were rapidly accumulating a pool of carbon species, easily hydrogenated during TPH experiments. Small amounts of ethane were also observed during the TPH experiments carried out on long-term aged catalysts (9). Other types of carbon deposits, much more stable and developing at the outside of the Ni particles, were shown to accumulate slowly with time-on-stream and were considered as contributing to the catalyst deactivation.

The present study focuses more specifically on the reaction mechanism. Non-steady-state and steady-state isotopic transient experiments were carried out in order to identify both the intermediate species I directly involved in the syngas formation (i.e., participating as active intermediates in the catalytic cycle) and the carbon species slowly accumulating via side reactions. They revealed accumulation and/or release of various amounts of carbon and oxygen deposits, depending on the transient conditions (Table 4). These amounts were also expressed as atomic ratios I/N_s^0, Ni_s^0 being the concentration of surface nickel atoms calculated from the nickel dispersion and reduction degree measured at each step of the catalytic run by magnetic measurements.

State of the Working Surface under Non-Steady-State Conditions

$He \rightarrow CH_4/CO_2/He/Ar$. During the initial contact of the catalyst with the reacting mixture, it was shown from the uptake of methane and carbon dioxide corrected for the release of carbon monoxide that around 170 μmol/g_{cat} of carbonaceous species were accumulating on the solid. This corresponded to a C/Ni_s^0 ratio equal to 2.4. No detectable accumulation of reversible hydrogen was observed during this start-up period. This is in line with the fact that no hydrogenated deposits were detected after a short time-on-stream by DRIFT analysis. As a matter of fact, the only hydrogenated carbon deposits, observed by DRIFT, appeared only after long time-on-stream (Fig. 8b). Note that the dehydrogenated character of the initial carbon deposits on a Ni catalyst is in contrast with the observations reported on supported Pd and Pt catalysts (2, 3), indicating the presence of adsorbed hydrogen under similar conditions of dry reforming of methane.

$CH_4/CO_2/He/Ar \rightarrow CO_2/He$. Large amounts of CO were released from the surface under pure CO_2 atmosphere showing that carbon dioxide could react directly with the carbon deposits to CO. Quantitatively, the amount of produced CO (514 μmol/g_{cat}) corresponded to about three times the amount of initially accumulated C deposits (170 μmol/g_{cat}). Taking into account some extra accumulation of carbon between the initial uptake and the present transient, the amount of CO produced can be well explained by the reverse Boudouard reaction ($CO_2 + C \rightarrow 2\ CO$), allowing the initial carbon deposits to be oxidised by CO_2. The slight deactivation observed after this transient could come from some particle sintering occurring under the oxidising CO_2/He atmosphere.

$CH_4/CO_2/He/Ar \rightarrow CH_4/He$. A significant residual production of hydrogen (1538 μmol/g) corresponding to a conversion of 820 μmol/g_{cat} of methane was observed during this transient step (Fig. 3, Table 4). This demonstrated that a molecule of methane was probably decomposed into two hydrogen molecules and one carbon atom, the latter reacting with the nickel phase to form bulk carbide species, as suggested by the marked decrease of the ferromagnetic

signal. However, the amount of nickel carbide which would result from this methane cracking (i.e., 820 μmol of Ni_3C/g_{cat}) was more than three times the amount corresponding to the theoretical transformation of the whole nickel phase into bulk carbide (calculated as 227 μmol of Ni_3C/g_{cat}). Furthermore, it was observed from the magnetic measurements carried out after 1 h treatment under methane rich atmosphere that only one-third of the nickel phase was no more ferromagnetic (decrease of the ferromagnetic signal from 95 to 68%). It may therefore be concluded that only a fraction of the Ni particles was transformed into bulk carbide, other forms of carbon deposits being also formed outside the Ni particles as observed by TEM analysis (9). Note, however, that under the present conditions, i.e., in the absence of CO_2 or H_2O, this carbon deposition stopped rapidly. This underlined that the methane decomposition was markedly enhanced in the presence of the coreactant CO_2 or H_2O. No deactivation was observed after this treatment under methane rich atmosphere. It can be deduced from these results that: (i) the actual active phase under reforming conditions was close or similar to a nickel carbide phase, and (ii) the outer carbon deposits formed only from methane decomposition were not deactivating, as already proposed in Part I of the study.

State of the Working Surface under Steady-State Conditions

The concentration of the reacting intermediates I under steady-state conditions was obtained from the $^{12}CH_4/^{12}CO_2/He \rightarrow {}^{13}CH_4/^{12}CO_2/He/Ar$ SSITKA (Table 4). It was found to correspond to a I/Ni^0_s ratio equal to 0.53, a very low value as compared with the large amounts of carbon deposits measured under non-steady-state conditions. This concentration of steady-state active intermediates corresponds approximately to the C saturation limit of nickel surfaces observed on single crystals (15, 16). Note also that the formation of a surface carbide with the stoichiometry $C/Ni^0_s = 1/3$ was proposed for the reaction of CO hydrogenation into methane over Ni/SiO_2 catalysts in the temperature range 250–400°C (17, 18).

A further analysis of the data in Table 4 revealed that the largest part of the reacting adspecies were related to the formation of CO (about 80% of the total amount of adspecies). This was calculated from the delay between the labeled methane (almost overlapping the inert tracer) and the labeled carbon monoxide. The methane overall conversion was found to be largely irreversible from two pieces of independent experimental evidence: (i) the carbon isotopic composition of the unconverted methane was shown to be only partly scrambled (14% ^{12}C and 86% ^{13}C) when the reactor was fed with the $^{13}CH_4/^{12}CO_2/He/Ar$ mixture (Table 5), and (ii) the ratio of H/D exchange (reversible activation) to converted methane into CO (irreversible activation) was very low at both 600 and 700°C. Therefore the above accumulation of CO precursors could be assigned to the direct conversion of methane into carbon monoxide. The remaining part of the reacting intermediates corresponded to the delay between the inert tracer and the CO_2 transients. Such a delay would actually reflect the reversible accumulation of CO_2 precursors on the catalyst surface. The reversible character of carbon dioxide activation was also proved by its fast interconversion with CO as deduced from the scrambled isotopic composition of the two gases at the reactor outlet under steady-state $^{13}CH_4/^{12}CO_2/He/Ar$ feeding regime (Table 5).

From the flash TPO experiment carried out after 10 min under $^{13}CH_4/^{12}CO_2/He$ mixture, two types of carbonaceous deposits were revealed (Table 6): one which was easily oxidised (at 500°C) corresponded to 47.2 μmol/g_{cat}, i.e., to a ratio C/Ni^0_s equal to 0.53, and a second, more stable towards oxygen (oxidised between 500 and 800°C), which corresponded to 37.6 μmol/g_{cat}. The easily oxidised carbon deposits may reasonably be assigned to the reacting intermediates identified from SSITK analysis for two reasons: (i) both amounts were similar (C/Ni^0_s equal to 0.53) and (ii) their isotopic composition revealed that a large part of these deposits was formed of ^{13}C (76%, Table 6). This agrees perfectly with the fact that a large part of the active adspecies were shown to be CO precursors, arising from the largely irreversible activation of methane (SSITKA experiments).

The less easily oxidised carbon deposits detected by TPO would accordingly correspond to slowly accumulating species which would transform progressively with time-on-stream into carbon whiskers and/or carbon veils as observed by TEM (Part I). Their isotopic composition was found to be 60% ^{12}C and 40% ^{13}C (Table 6), i.e., rather close to the isotopic composition of the gaseous CO and CO_2 effluents when the reactor was fed with $^{13}CH_4/^{12}CO_2/He/Ar$ (Table 5). This would indicate that these less reactive deposits could arise both from CH_4 and from CO_2 activation on the catalyst. By referring to the numerous models proposed in the literature about carbon whisker formation under steam reforming conditions (19), a similar growth process via carbide species migration could be proposed under dry reforming conditions: part of the carbide-like active species would migrate through the nickel particles to be slowly released as whiskers or carbon veils. The possible site requirement for the formation of these different types of carbon deposits will be discussed later.

The last key information about the working surface was provided by *in situ* DRIFT spectroscopy. No adsorbed CO and OH vibrations were detected at 700°C, indicating that neither Ni–CO nor Ni–OH adspecies formed significant pools on the reacting surface under reforming conditions (Fig. 6b). In contrast, evidence of adsorbed CO was found at lower temperature (500°C) at low methane conversions. This strongly suggested that CO_2 could easily dissociate on

Ni particles into adsorbed CO and most probably adsorbed O, as already proposed in an infrared study of CO_2 activation on Ni/SiO_2 catalysts (13). The absence of adsorbed CO at 700°C would derive from a much lower residence time on the reacting surface, resulting in a negligible surface accumulation.

Mechanistic Scheme

From the above description of the working surface under non-steady-state and steady-state conditions, several mechanistic steps can be proposed, in relation to the surface occupancy:

(i) The first step of methane activation consists of a reversible reaction between gaseous molecules and surface sites S_1, leading to adsorbed carbon and gaseous hydrogen according to

$$CH_4 + S_1 \rightleftharpoons C_{ads} + 2H_2. \quad [1]$$

This corresponds under steady-state conditions to the formation of a pool of around one monolayer of carbide-like active intermediate species. Within this step, the intermediate formation of hydrogenated species CH_x and a fast gas/surface hydrogen equilibrium have to be considered in order to account for the observed H/D exchange reactions (Table 3). However, no evidence of significant accumulation of CH_x or H_{ads} species was found. A marked KIE corresponds to this reversible part of the methane activation, as expected for a step involving several C–H bond breakings (onward) and formation (backward). To summarise, step [1] can be considered under the present conditions as a fast step, largely reversible at 700°C and leading solely to the accumulation of dehydrogenated carbon monomers.

(ii) Carbon dioxide was also found to be in fast equilibrium with the reacting surface and easily interconverting with carbon monoxide. Assuming that the reacting surface was essentially the carbide-like phase formed from step [1]. this step could be written in a first approximation as an overall equilibrium, as assumed by Erdöhelyi *et al.* (7):

$$CO_2 + C_{ads} \rightleftharpoons 2CO + S_1. \quad [2]$$

Actually, the *in situ* characterisation of the working surface led us to propose that this equilibrium would most probably result from two elementary steps which would account for the CO formation:

(a) The dissociative adsorption of CO_2 on a site S_2 leading to surface oxygen and CO. The latter would be immediately released into the gas phase, as indicated by the IR study and in accordance with studies of CO_2 activation on nickel, reviewed by Solymosi (20):

$$CO_2 + S_2 \rightleftharpoons CO + O_{ads}. \quad [3]$$

(b) The reaction of surface carbon monomers (arising from step [1]) with surface oxygen atoms (arising from step [3]) into CO immediately released into the gas phase:

$$C_{ads} + O_{ads} \rightarrow CO + S_1 + S_2. \quad [4]$$

Step [3] has to be considered as highly reversible and fast in order to explain the isotopic equilibrium established between CO_2 and CO. It accounts for the delay corresponding to the transient CO_2 curve (Fig. 4b).

In contrast, step [4] cannot be considered as fast, since it allows the accumulation of the surface intermediates revealed by various independent techniques (SSITKA, TPO, TPH). It can neither be considered as highly reversible since almost no $^{12}C/^{13}C$ isotopic scrambling was observed for this pool of active surface carbons (Table 5). Moreover, no isotopic effect was observed for the overall methane and carbon dioxide conversion, indicating that the rate determining step (RDS) of the process does not involve C–H bond breakage or formation. Accordingly, step [4] can be proposed as rate limiting. This could be due to the fact that it requires surface migration of adspecies like adsorbed O and C. As a matter of fact, the surface diffusion which generally presents a lower activation energy than adsorption or desorption steps is expected to be relatively unfavoured at high temperature.

(iii) Although not quantified precisely due to significant non-catalytic chromatographic effects, the kinetic role of water has also to be taken into account. For all the transient experiments, a kinetic behaviour close to that of CO_2 was observed. Evidence of an isotopic H/D scrambling was also provided during CH_4/CD_4 equilibration experiments. This strongly suggests that water interacts reversibly with the catalytic surface via an adsorption/desorption equilibrium in a similar way as carbon dioxide:

$$H_2O + S_2 \rightleftharpoons O_{ads} + H_2. \quad [5]$$

This equilibrium is consistent with the absence of hydroxyl group accumulation, as indicated by *in situ* DRIFT, and for the absence of surface hydrogen accumulation. Moreover, the combination of steps [3] and [5] represents the WGS equilibrium, which was shown to be achieved under the present reaction conditions (8).

Configuration of the Active Sites

From this mechanistic scheme, it may be deduced that the active site for methane activation (S_1) requires at least two adjacent free Ni atoms to accommodate the carbon monomer considered as a carbide-like species (step [1]). From previous studies devoted to methane adsorption over the same Ni/SiO_2 catalyst, it was shown by high-field magnetic methods (21) and by a kinetic investigation of deuterium exchange (22) that methane adsorption at temperatures higher than 130°C involved the complete cracking of

the molecule as follows:

$$CH_4 + 7Ni \rightarrow Ni_3C + 4Ni{-}H. \quad [6]$$

This scheme required a site of seven adjacent Ni atoms to accommodate both the carbon and the hydrogen adspecies. Under the present reforming conditions, no measurable amounts of hydrogen were accumulating on the surface. However, a close site configuration could be considered since (i) a direct and concerted process of C–H bond cleavage and H_2 recombination is unlikely, and (ii) transient formation of Ni–H bonds (corresponding to intermediate steps within the equilibrium [1]) may occur without leading to a stable occupancy of the surface by atomic hydrogen; in contrast, the CO_2 activation would be less demanding, since it occurs on a site S_2 formed of only one surface Ni atom for accommodating the oxygen atoms (step [3]). A second Ni atom could also be considered for the transient formation of a Ni–CO adspecies. As a matter of fact, though not detected by DRIFT spectroscopy, this short lifetime intermediate would most likely be linearly adsorbed CO in line with its high instability.

On the basis of the above assumption of different Ni atom ensembles for either methane or carbon dioxide activation, the actual surface occupancy for both processes can tentatively be evaluated. Let us consider the surface concentrations of the intermediate adspecies expressed as I/Ni_s^0 ratios in Table 4. By considering the number of surface Ni atoms corresponding to each type of site (7 for methane and 2 for carbon dioxide), the fraction of surface corresponding to methane adsorption and to carbon dioxide activation would be proportional to 0.43×7 and to 0.10×2, respectively. This would give 94 and 6% of the Ni surface dedicated to methane and carbon dioxide activation, respectively. Despite the uncertainties of this evaluation (including the fact that water activation should also be considered), this large difference between surface occupancies could reflect some structure effect for these reactions. The demanding methane activation would possibly be favoured on the smooth planes of the nickel particles. In contrast, the less demanding carbon dioxide activation would preferentially proceed on the rough parts of the particles where highly coordinatively unsaturated (CUS) nickel atoms dominate. As a matter of fact, recent experimental IR data were obtained at the laboratory, suggesting that corner and edge Ni atoms form more easily Ni–O bonds than plane atoms (unpublished results). Experiments aimed at investigating this hypothesis of structure sensitivity are in progress. Indeed the competitive adsorption of methane and carbon dioxide on the same sites remains a plausible alternative to be considered.

REFERENCES

1. Tsang, S. C., Claridge, J. B., and Green, M. L. H., *Catal. Today* **23**, 3 (1995).
2. Solymosi, F., Kutsan, G., and Erdöhely, A., *Catal. Lett.* **11**, 219 (1991).
3. Huder, K., *Chem.-Ing.-Tech.* **63**, 376 (1991).
4. Mark, M. F., and Maier, W. F., *Angew. Chem. Int. Ed. Engl.* **33**, 1667 (1994).
5. Rostrup-Nielsen, J. R., and Bak Hansen, J.-H., *J. Catal.* **144**, 38 (1993).
6. Bodrov, I. M., and Apel'baum, L. O., *Kinet. Katal.* **8**, 379 (1967).
7. Erdöhelyi, A., Cserényi, J., and Solymosi, F., *J. Catal.* **141**, 287 (1993).
8. Swaan, H. M., Kroll, V. C. H., Martin, G. A., and Mirodatos, C., *Catal. Today* **21**, 571 (1994).
9. Kroll, V. C. H., Swaan, H. M., and Mirodatos, C., *J. Catal.* **161**, 409 (1996).
10. Mirodatos, C., *Catal. Today* **9**, 83 (1991); Mirodatos, C., *in* "Catalyst Characterisation" (B. Imelik and J. C. Védrine, Eds.), p. 661, Plenum, New York, 1994.
11. Martin, G. A., Mirodatos, C., and Praliaud, H., *Appl. Catal.* **1**, 367 (1981).
12. Melander, L., "Isotopic Effects on Reation Rates." Ronald Press, New York, 1960.
13. Martin, G. A., Primet, M., and Dalmon, J. A., *J. Catal.* **53**, 321 (1978).
14. Socrates, G., "Infrared Characteristic Group Frequencies." Wiley, New York, 1980.
15. Gauthier, Y., Baudoing-Savois, R., Heinz, K., and Landskron, H., *Surf. Sci.* **251/252**, 493 (1991).
16. Kilcoyne, A. L. D., Woodruff, D. P., Robinson, A. W., Lindner, Th., Somers, J. S., and Bradshaw, A. M., *Surf. Sci.* **253**, 107 (1991).
17. Mirodatos, C., Dalmon, J. A., and Martin, G. A., *in* "Catalysis on the Energy Scene" (S. Kaliaguine and A. Mahay, Eds.), p. 505. Elsevier, Amsterdam, 1984.
18. Mirodatos, C., Brum-Pereira, E., Gomez Cobo, A., Dalmon, J. A., and Martin, G. A., *Top. Catal.* **2**, 183 (1995).
19. Rostrup-Nielsen, J. R., *in* "Catalysis, Science and Technology" (J. R. Anderson and M. Boudart, Eds.), Vol. 5, p. 1. Springer-Verlag, Berlin, 1984.
20. Solymosi, F., *J. Mol. Cat.* **65**, 337 (1991).
21. Martin, G. A., and Imelik, B., *Surf. Sci.* **42**, 157 (1974).
22. Leach, H. F., Mirodatos, C., and Whan, D. A., *J. Catal.* **63**, 138 (1980).